

# Physical Insights and Test Stand Results for the LANSCE H<sup>-</sup> Surface Converter Source

Joseph Sherman, Edwin Chacon-Golcher, Ernest G. Geros, Edward Jacobson, Patrick Lara, Bruce J. Meyer, Peter Naffziger, Gary Rouleau, Stuart C. Schaller, Ralph R. Stevens, Jr., and Thomas Zaugg

*LANSCE Division, Los Alamos National Laboratory, Los Alamos, NM87545*

Abstract. The Los Alamos Neutron Science Center (LANSCE) H<sup>-</sup> surface converter source upgrade project has been ongoing for several years to reach 25-40 mA current with 7( $\pi$ cm-mrad) lab emittance (95% beam fraction). The duty factor is 12% (120 Hz, 1ms pulse length). Summary test stand results and interpretations for a six filament axial extraction H<sup>-</sup> source are presented. This source did produce 40-mA H<sup>-</sup> current, but with unacceptable emittance growth. More recently a fourth, modified LANSCE H<sup>-</sup> production source with radial H<sup>-</sup> extraction system has been constructed, and is presently undergoing tests. Currents up to 25mA H<sup>-</sup> have been observed with 20% emittance growth. This emittance growth may be acceptable for 800 MeV linac operations. A summary of physical principles of emittance growth mechanisms and converter physics are given.

## INTRODUCTION

Significant upgrades to the LANSCE 800-MeV linac and Proton Storage Ring (PSR) operations can be realized by development of an H<sup>-</sup> ion source with laboratory emittance of 7( $\pi$ cm-mrad) at 95% beam fraction with 20-40mA H<sup>-</sup> current. The source beam energy is 80keV and the duty factor (df) is 12%. A six-filament version of the surface converter source with axial H<sup>-</sup> beam extraction was developed in a collaborative effort between Lawrence Berkeley National (LBNL) and Los Alamos National Laboratories (LANL)[1]. Although this source did produce 40-mA H<sup>-</sup> current, an unexpected emittance growth factor of 2.5 made these higher current beams unacceptable for LANSCE operations[2]. A subsequent decision was made to fabricate and develop a fourth production source to produce 25-mA H<sup>-</sup> current with an emittance growth of no greater than 20%[3]. The source upgrade technology would be used in the 750-keV H<sup>-</sup> injector B at LANSCE.

Experiments and analysis on the six-filament axial extraction source will be reviewed in the next section. Evidence is given that at the higher discharge power characteristic of this source, two beams are formed at extraction. The two beams originate from surface (converter electrode) and volume processes. The third section summarizes recent work completed on the fourth production source with radial extraction. Effort is directed at increasing the H<sup>-</sup> current without significantly increasing the discharge power, thus avoiding the two-beam emittance growth mechanism. All beam measurements were made on the LANSCE Ion Source Test Stand (ISTS), which is now computer controlled and may be operated on a 24 hour, 7-day/week bases.

## SIX FILAMENT AXIAL EXTRACTION SOURCE

Figure 1 shows a photo of the copper axial extraction  $H^-$  source. Most of the six-filament development was done with this source. A higher current column with focus electrode was developed at LBNL for 80keV, 40-mA operations[4], although many measurements were also

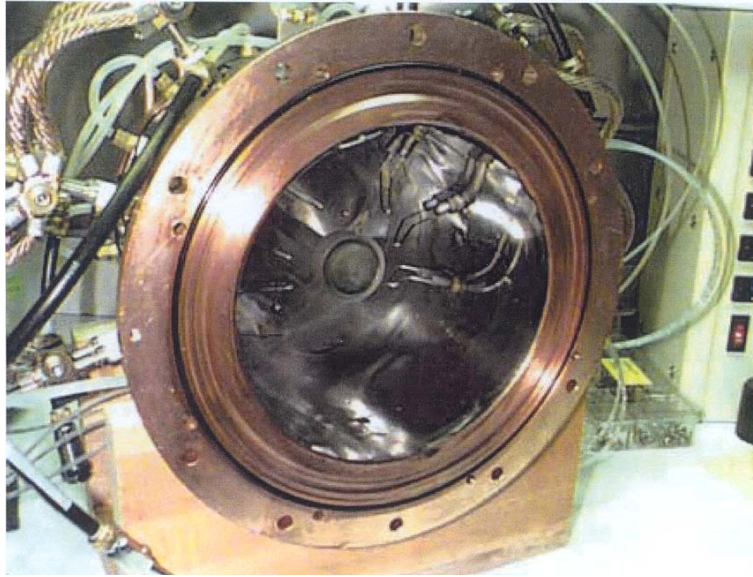


Fig. 1. Photo of the copper prototype axial source with the electron repeller assembly and emission aperture (Pierce electrode) mount plate removed. The molybdenum converter with its quartz insulator and six tungsten filaments are visible.

done with the LANSCE production column[5]. (A scaled drawing for the LBNL accel column is shown below in Fig. 5.)  $H^-$  is produced at the cesiated converter surface[6], and subsequently accelerated towards the emission aperture by the  $-250$  to  $-300V$  bias of the converter electrode. The axial geometry permits a full-line, cusp-magnet configuration for plasma confinement, and the copper housing provides good temperature control even at the high discharge powers used in the six-filament source. No temperature related problems were observed in the copper source operation. The converter surface has a curvature radius  $\rho_{cnv} = 12.5cm$  to focus  $H^-$  ions toward the emission aperture. Emission aperture radii were either  $r_p = 0.8$  or  $0.5cm$ . The filaments operate in an emission-limit mode with up to  $175A$  discharge current in hydrogen-cesium gases where the  $H_2$  gas pressure is  $3-7mTorr$ . All measurements were made at  $80keV$  on the ISTS, shown in Fig. 2. The ISTS is a reproduction of the LANSCE injector B  $80-keV$  beam system[7]. Slit and collector emittance stations are located immediately after  $80-kV$  column, between the two focus solenoids, and near the end of the LEBT. These are labelled emittance stations 1, 2, and 3 in Fig. 2. The end of the LEBT corresponds to the injector B  $670-kV$  column injection point. Beam current measurements are made between the solenoids (beam current transformer), and then at the end of the LEBT in a Faraday cup.

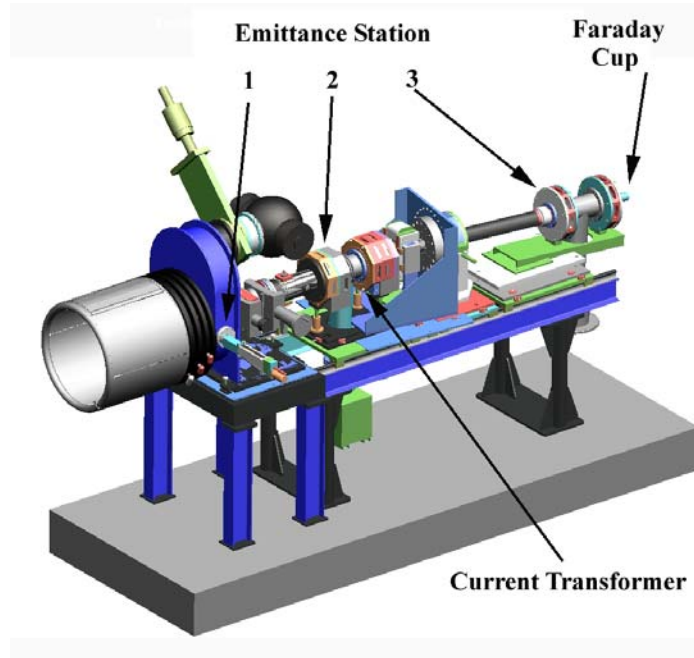


Fig. 2. Shows the ISTS and low-energy beam transport system (LEBT) diagnostics used in these measurements.

Figures 3(A) and 3(B), respectively, show  $H^-$  beam current transformer measurements for  $r_p = 0.8$  and  $0.5\text{cm}$ . Four different repeller magnet assemblies were used in this source development[1,2]: line cusp magnets, two ring solenoid magnets with on-axis fields of 500 and 250G, and an undulator magnet comprised of two dipole magnets. The  $e/H^-$  ratios for the line cusp, ring solenoid, and undulator repeller magnets gave  $e/H^- = 4, 2.4,$  and  $1,$  respectively. Fig. 3(A) shows that all four repeller magnet configurations gave  $40\text{mA}$   $H^-$  current. The solid curve shows the  $H^-$  beam current follows an approximate square root dependence on the discharge

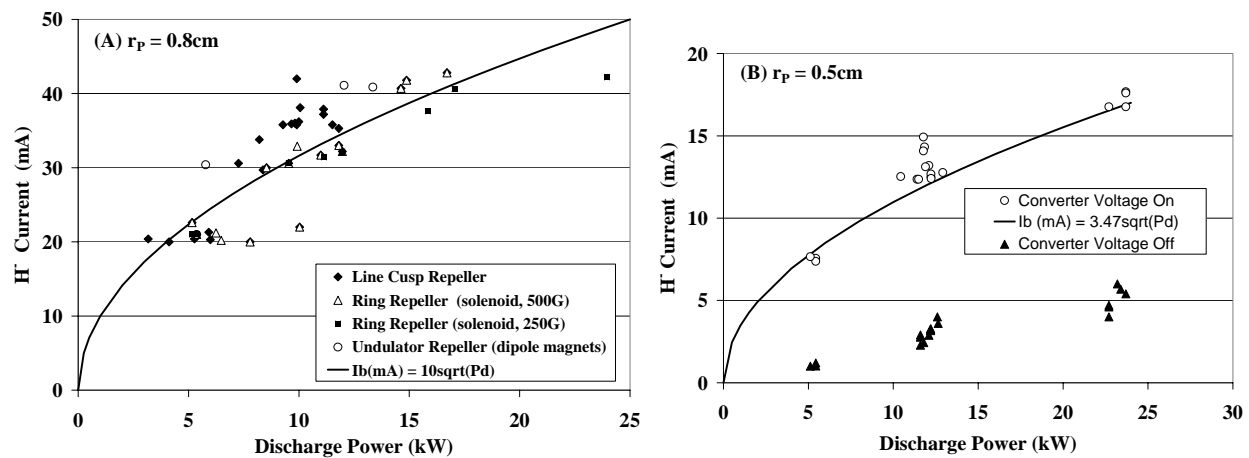


Fig. 3. (A) Shows  $H^-$  current measurements made with four different repeller magnets in place with the  $r_p = 0.8\text{cm}$  emission aperture. (B)  $H^-$  current measurements made with  $r_p = 0.5\text{cm}$ , and with the converter voltage turned on and off. All measurements made at  $80\text{keV}$  beam energy.

power. The discharge voltage was typically  $-140\text{V}$ . Data in Fig. 3(B) were taken with the converter voltage on (open symbol), and then with the converter voltage off (filled symbols). The undulator repeller configuration was used, and the data again shows  $H^-$  currents with

converter on following a square root dependence on discharge power. Fig. 3(B) also shows a linear increasing  $H^-$  current with converter voltage off, thus suggesting  $H^-$  production mechanisms other than  $H^-$  surface conversion are increasing with discharge power. The ratio of the normalizing coefficients for the  $H^-$  current dependence on discharge power is  $10/3.47 = 2.9$ , which nearly equals the ratio of Pierce aperture radii, squared,  $(8/5)^2 = 2.6$ . Thus the emission aperture appears to be uniformly illuminated by  $H^-$  from the plasma with maximum  $H^-$  current density  $j_{H^-} = 21\text{mA/cm}^2$ .

Fig. 4(A) shows a summary of the total lab emittance ( $\epsilon_l$ ) extracted from the slit and collector phase-space measurement gear. The area is calculated at the 2% threshold level, which usually corresponds to beam fractions greater than 98%. The solid symbols show data from

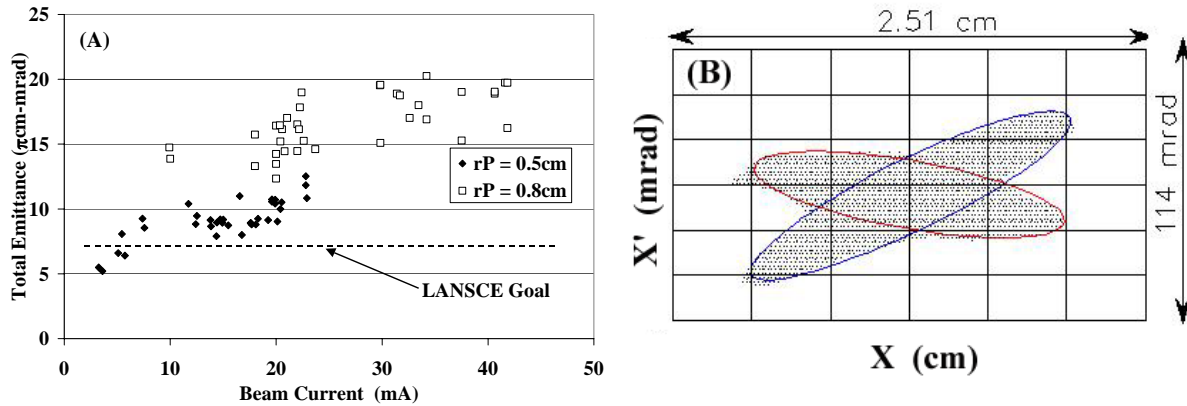


Fig. 4. (A) Summary of emittance measurements made with the axial copper source using  $r_p = 0.5$  and  $0.8\text{cm}$  emission apertures. (B) Slit and collector phase space scan at ISTS emittance station 3. The full scales on the phase space scan are shown. The ellipses drawn on the data are discussed in the text.

$r_p = 0.5\text{cm}$ , while the open symbols show the emittance data from the  $r_p = 0.8\text{cm}$  aperture. Above approximately  $16\text{mA}$   $H^-$  current, there is an emittance increase, which makes tuning of the LANSCE injector B  $750\text{keV}$  beam line increasingly difficult[8]. The emittance data in Fig. 4(A) are selected from the three emittance stations in the  $80\text{keV}$  LEPT while the ion source was operating with the  $80\text{kV}$  LBNL column. The emittance limits based on the converter source admittances (see refs. [1,2] and below) for  $r_p = 0.5$  and  $0.8\text{cm}$  sources are respectively  $5.4$  and  $7.5(\pi\text{cm-mrad})$ . Thus most of the measured emittances are greater than the source admittance limits. Fig. 4(B) shows a  $30\text{-mA}$  emittance scan acquired at station three with the LANSCE  $80\text{keV}$  column. The total emittance derived from this phase-space scan is  $18(\pi\text{cm-mrad})$ . The dots represent current intensity at the 2% threshold analysis level. A two-beam structure is particularly evident in Fig. 4(B). Superposition of two beams formed at extraction is thought to be the dominant emittance growth mechanism when the surface converter source is operated at higher discharge power.

A theoretical estimation of the two-beam emittance growth mechanism may be made using the  $H^-$  plasma option model of the PBGUNS code[9,10]. The PBGUNS plasma model for the high current accel column is shown to scale in Fig. 5. Relative to ground potential, this simulation has the Pierce electrode ( $r_p = 0.8\text{cm}$ ) at  $-80\text{kV}$ , the extractor electrode at  $-50\text{kV}$ , the focus electrode at  $-75\text{kV}$ , the ion trap electrode at  $5\text{kV}$ , and the ground electrode at  $0\text{ kV}$ . The

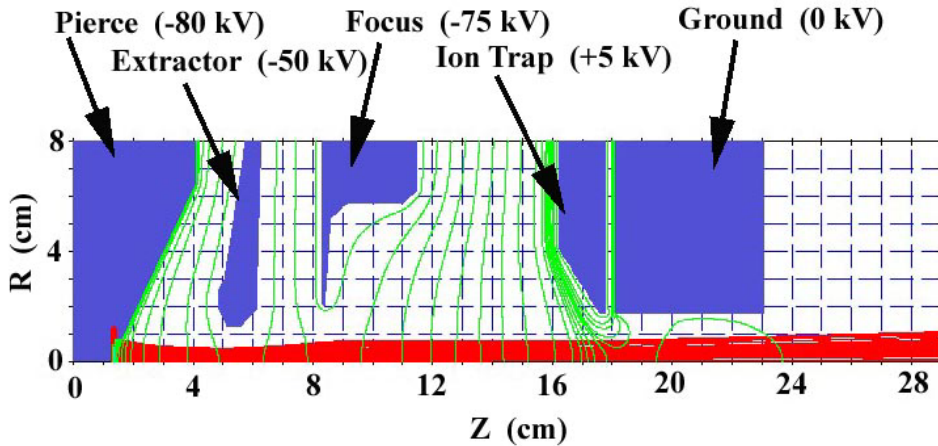


Figure 5. Shows a scaled drawing of the LBNL accel column with predicted trajectories for a 30-mA  $H^-$  beam. Electrode potentials relative to local ground are given.

code calculates a self-consistent sheath (cf ref. [10] for an example of the sheath location and shape). The accelerated  $H^-$  beam current is 30mA, and is composed of injected  $H^-$  ions with 50% 12eV (energy characteristic of volume  $H^-$  in the pre-sheath), and 50% 300eV  $H^-$  ions (energy characteristic of surface converter  $H^-$ ).

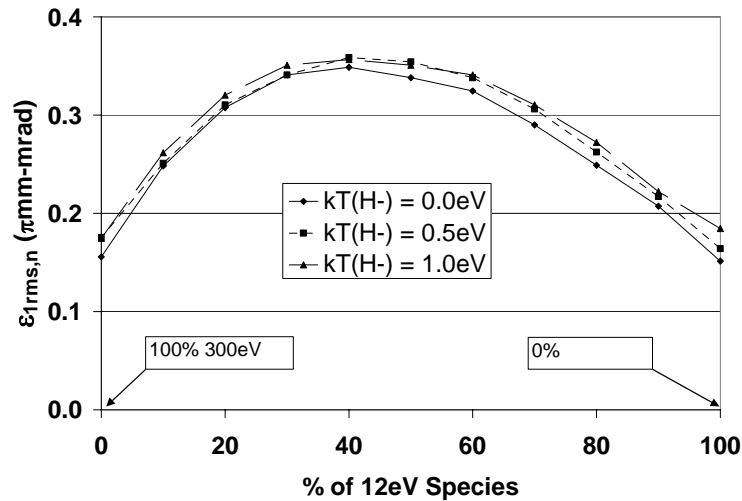


Fig. 6. Predicted  $\varepsilon_{1rms,n}$  vs % of 12eV species in 30 mA  $H^-$  current. The remaining current % is in the 300eV injected species.

The predicted one rms normalized emittances ( $\varepsilon_{1rms,n}$ ) as a function of the % input 12eV (volume)  $H^-$  species is shown in Fig. 6. The relation between normalized emittances and total lab emittances [1] for the Fig. 4(A) data is  $\varepsilon_l = 7(\varepsilon_{1rms,n})/\beta$ , where  $\beta = 0.13$  is the relativistic velocity factor of 80keV  $H^-$  ion. A maximum emittance growth by the PBGUNS two-beam model is factor 2.2, which agrees with the emittance growth shown in Fig. 4(A). The maximum predicted  $\varepsilon_{1rms,n} = 0.35$  ( $\pi\text{mm-mrad}$ ), which corresponds to  $19(\pi\text{cm-mrad})$  lab total emittance, is also in good agreement with maximum emittances of Fig. 4(A). The three curves in Fig. 6 are parametric in plasma  $H^-$  temperature. Increasing the  $H^-$  temperature from 0 to 1eV does not

describe the observed emittance growths within this model. An emittance growth calculation derived from mismatch formalism[11] may be attempted. The ellipses drawn in Fig. 4(B) have the following Courant-Snyder parameters: for the convergent beam;  $\alpha_c = .795$ ,  $\beta_c = .0779$  (cm/mrad), and for the divergent beam;  $\alpha_d = -2.45$ ,  $\beta_d = .0775$ (cm/mrad). An emittance growth factor of 3.5 is derived, which on the  $1\epsilon_{rms,n}$  scale of Fig. 6 corresponds to 0.45 ( $\pi$ mm-mrad). This approach appears to overestimate emittance growth.

## TWO FILAMENT RADIAL EXTRACTION SOURCE

A fourth radial extraction (LANSCE production) source has been assembled for development purposes. Goals are to produce a 25mA  $H^-$  source, < 85mA total pulsed current, < 20% emittance growth as compared to operations source, and 12% df (120Hz, 1ms). The specification of 85mA total pulsed current implies  $e/H^-$  ratio < 2.4. Reasons for this approach are: (1) the present LANSCE 80-kV accel column is thought to be sufficient for 25-mA  $H^-$  beam production[5], (2) there is tremendous operational experience with the radial extraction source, (3) there is clear upgrade path to 25-mA facility operation, and (4) higher power operation available in the 6-filament source does not appear to be desirable short-term solution for LANSCE injector B. A side view photo of the radial production source is shown in Fig. 7. The

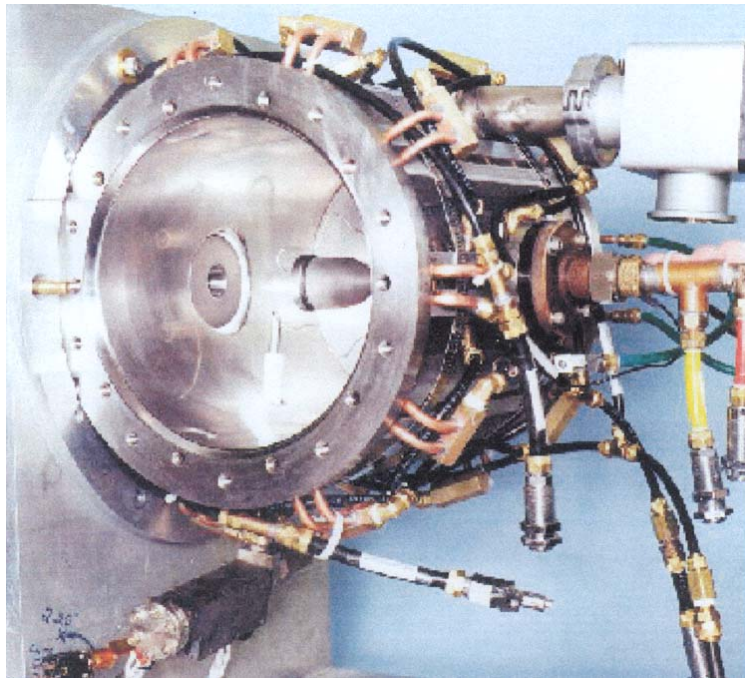


Fig. 7. LANSCE production source. Present development is using a simple modification of this source.

converter electrode is seen near the center of the source with the cesium oven feed tube just below. Both of these components are made of molybdenum. The electron repeller assembly is located opposite the converter electrode on the stainless steel wall. The  $H^-$  converter beam (250 – 300eV) is extracted radially through a broken line cusp magnet row. This source was developed 20 years ago for the proton storage ring at LANSCE[12,13].

Table 1 contains summary data relating to the development program. The first column is a source parameter number, the second column contains the source parameter, the third column the

Table 1. Comparison of LANSCE production source, status of the development source, and the development goal.

	<i>Ion Source Parameter</i>	<i>Production Source</i>	<i>Development Status</i>	<i>Development Goal</i>
1	$r_p$ (cm)	0.50	0.60	TBD**
2	$r_{rep}$ (cm)	0.64	0.86	0.86
3	$r_{cnv}$ (cm)	1.9	1.9	TBD
4	$\rho_{cnv}$ (cm)	12.5	12.5	TBD
5	Admittance (cm-mrad)	304	379	TBD
6	$B_c$ (kG)	2.0	3.4	TBD
7	Electron repel ( $I_{H^-}$ ) <sub>max</sub>	Line cusp	Line cusp	TBD
8	Discharge power (kW)	8	7.6	8
9	( $I_{H^-}$ ) <sub>max</sub> (mA)	18	25	25
10	e/H- ratio (line cusp)	3.0	5.9	2.4
11	Electron repel (for $\epsilon_1$ )	Line cusp	PM solenoid	TBD
12	e/H <sup>-</sup> ratio (ring PM)		4	2.4
13	$\epsilon_1$ ( $\pi$ cm-mrad), measured	7	8-9*	8.4

\*( $I_{H^-} = 20$ mA), \*\*TBD = to be determined

production source parameter value, the fourth column the development source status, and the last column the development source goal. The development approach is to increase the emission aperture to  $r_p=0.6$ cm, thus increasing the emission area by a factor 1.44. The repeller aperture,  $r_{rep}$ , is also increased in the development source to prevent converter beam interception on this electrode. The production source typically produces 16-18mA  $H^-$ , thus the new source should produce 23-26mA  $H^-$ . This procedure maintains constant discharge power in the new source, thus filament lifetime between the two sources should be the same, and the 28-day accelerator run time between source recycles should be preserved. Additional development effort is being made to understand  $H^-$  production efficiency, especially as regards converter processes, with the goal of producing more  $H^-$  current at a fixed discharge power.

All results reported in this section have been obtained with the LANSCE production accel column. Fig. 8(A) shows the PBGUNS simulation for the LANSCE column with  $r_p = 0.6$ cm, limiting repeller aperture  $r_{rep} = 0.86$ cm, and the converter radius  $r_{cnv} = 1.9$ cm. The repeller housing can contain a variety of magnet geometries, and can also be biased to tens of volts to suppress electrons. The distance from the converter to the Pierce aperture is 12cm in this case – slightly less than the converter’s machined curvature radius  $\rho_{cnv} = 12.5$ cm. In a ballistic model of the source, no spreading of the converter  $H^-$  beam occurs, and the converter beam comes to a point focus near the Pierce aperture. This PBGUNS model uses the  $H^-$  sputter option where beam leaves the converter with 260eV and arrives at the emission aperture with uniform longitudinal energy. At 12eV sputter energy the repeller and Pierce apertures are fully illuminated with  $H^-$  beam, whereas at 6eV sputter energy the converter beam does not spread sufficiently to intercept the Pierce aperture. A discussion of the influence of sputter energy on simulations for this source is found in ref.[3]. The admittance diagram based on the

development source is shown in Fig. 8(B), and the area is  $A_{ad} = 379$  (cm-mrad) (cf Table 1, entry 5). For 300eV  $H^-$ ,  $\beta = 8.0 \times 10^{-4}$ , thus the limiting normalized emittance =  $\beta A_{ad} / \pi = 0.96$  ( $\pi$ mm-mrad). Converting this normalized emittance to 80keV laboratory emittance, one finds a lower

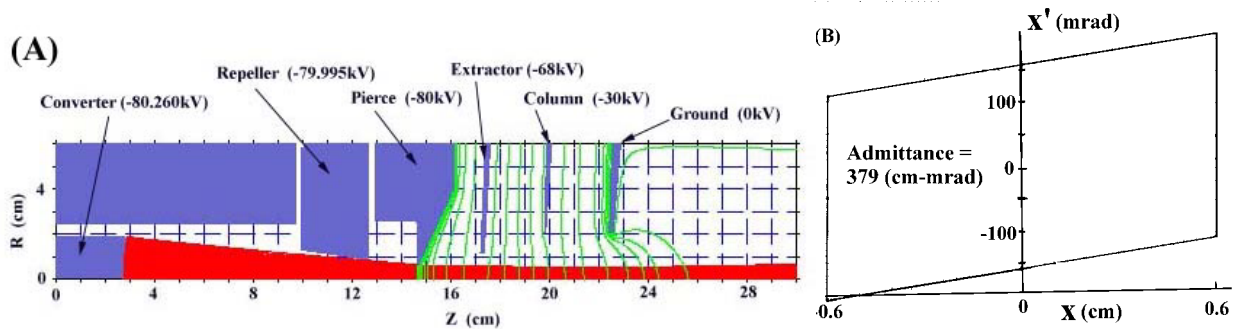


Fig. 8(A) PBGUNS simulation of the development source converter geometry and the LANSCE 80-kV accel column. Electrode potentials relative to local ground are given. (B) Converter source admittance diagram with  $r_p = 0.6$ cm.

emittance limit of  $7.4(\pi$ cm-mrad).

First operation of the development source led to unstable discharge voltages. This phenomenon has been previously observed in surface converter sources[14]. Stable arc

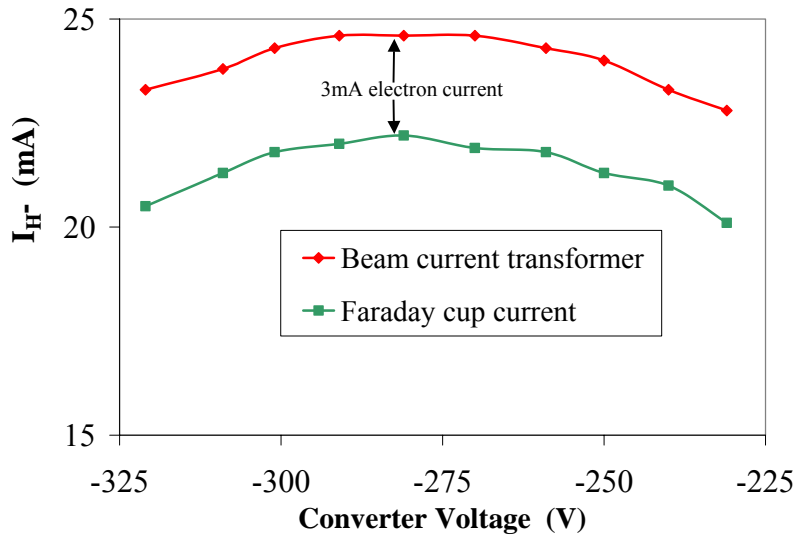


Fig. 9.  $H^-$  currents measured in the 80-keV LEBT. The beam current transformer located after solenoid 1, and the Faraday cup current measurement is made at the end of the LEBT.

discharge voltages at  $-190$ V were obtained by reducing the magnetic cusp confinement field at the source vacuum wall[3]. Using a line cusp magnet in the repeller assembly (cf entry 7 in Table 1), up to 25-mA  $H^-$  current has been obtained. The  $H^-$  currents measured in the beam current transformer after solenoid 1 and then in a Faraday cup at the end of the LEBT are shown in Fig. 9 as a function of the converter voltage. The  $H^-$  current has reached the 25-mA design at the beam current transformer, but decreases to 22mA at the Faraday cup (cf Fig. 2). The difference in current is thought to be residual electron current at the beam current transformer.

The  $e/H^-$  ratio was 5.9, see Table 1, parameter number 10. For the LANSCE injector B operations, this  $e/H^-$  ratio is too large by more than a factor two.

A permanent magnet (PM) ring solenoid (500G maximum on axis field) was installed in the development source repeller assembly. For the 6 filament source discussed above, this magnet configuration reduced the  $e/H^-$  ratio by about 50% [1,2]. On the two-filament development source, this magnet produced  $e/H^- = 4/1$ , a 32% reduction (cf line 12, Table 1). However the

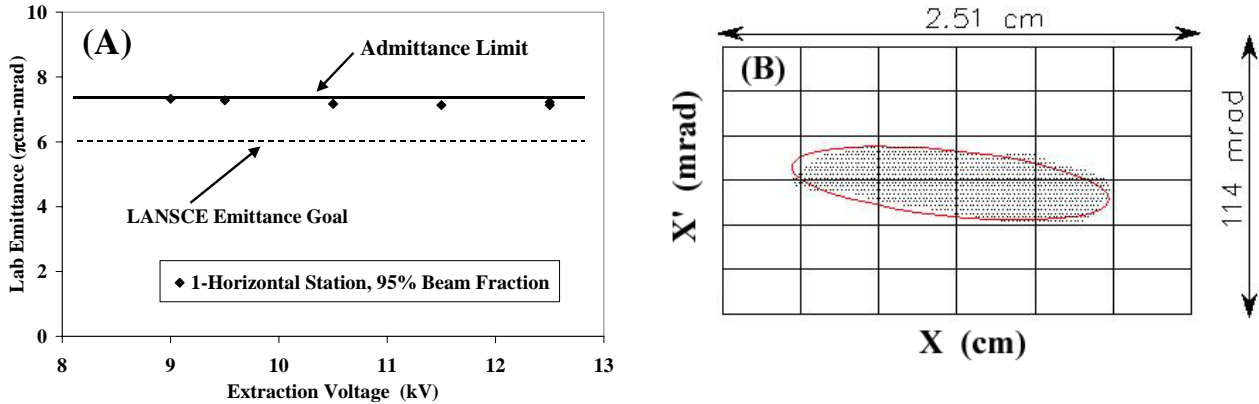


Fig. 10. (A). Measured emittances at station 1 on the ISTS. Taken on the development source for  $r_p = 0.6\text{cm}$  and 80keV beam energy. (B) Station 3 emittance scan for the development source corresponding to 17mA  $H^-$  current.

maximum  $H^-$  current at the ISTS current transformer was reduced to 20mA with 17mA being transported to the Faraday cup. Although this current is below the  $H^-$  specification (cf entry 9, Table 1), an emittance scan study was carried out at the three emittance stations as a function of the extractor electrode voltage. Emittance station one lab emittances shown in Fig. 10(A) are taken at 95% beam fraction. In a Gaussian beam emittance model, 95% beam fraction corresponds to six times the rms value. The development source results are near the predicted emittance minimum based on the admittance calculations (line 5, Table 1). The ratio of admittances in line 5, Table 1, for the development and production sources gives an emittance growth prediction =  $379/304 = 1.25$ , while the average measurements in Fig. 10(A) to the LANSCE emittance goal (dashed line in Fig. 10(A), production source emittance) gives the emittance growth = 1.2. The development source emittance limit of  $7.4(\pi\text{cm-mrad})$  is also shown in Fig. 10(A) as solid line. This prediction and emittance station 1 measurements are in agreement. Thus by source admittance limit arguments, there appears to be no unexpected emittance growth at station 1. At emittance station 2, the measured emittances are 8-9 ( $\pi\text{cm-mrad}$ ). This ISTS station corresponds to the injector B measurement which is typically  $7(\pi\text{cm-mrad})$ . Thus the emittance station 2 results are quoted in Table 1, line13. At emittance station 3, measured emittances are 8-10 ( $\pi\text{cm-mrad}$ ). The station 3 scan taken in the horizontal plane shown in Fig. 10(B) has laboratory emittance of  $8(\pi\text{cm-mrad})$ . Comparing Fig. 10(B) with Fig. 4(B) shows that the multi-beam component at this location is greatly reduced for the development source case. The ISTS focus solenoids had similar current settings for the Fig. 4(B) and 10(B) measurements. A systematic difference between the ISTS horizontal and vertical emittance results was noted earlier[3] in the development source work. Since the last development source data acquisition, a misalignment was found in the LEPT beam line, and this may be the cause of the asymmetric emittances [3] observed at stations 2 and 3.

Summarizing, the development source has met the design current (25mA) and design emittance, although the latter needs to be confirmed at the higher design current. The present

situation is that the  $e/H^-$  ratio is too great for injector B operations. Further efforts to reduce the  $e/H^-$  ratio are; first, reduce the magnetic field strength at the ion source wall; second, the wiggler (opposed dipole fields) repeller magnet may be tested in the development source; and third, careful measurements of the repeller voltage effect on  $e/H^-$  ratios can be made [15]. Modeling of cusp field confinement schemes has shown that reducing the confinement field will increase the source anode area[16,17], thus reducing electron current extraction at the emission aperture. The wiggler repeller magnet was used in the six-filament source, and it demonstrated a 75% reduction of extracted electron currents as compared to the line cusp repeller magnet[1,2].

A second approach for a more comprehensive solution to enhanced surface converter source performance is the improvement of the  $H^-$  production efficiency. This  $H^-$  surface converter source falls into the general category of cathodic surface plasma source (SPS)  $H^-$  production (cf. Fig. 1f in ref [18]). Total converter currents,  $I_{cnv}$ , in both the production and development sources are measured to be 4A. Secondary electron production coefficient  $\gamma = I_e/I^+$  at the cathode may vary from 1 to 7 while the secondary  $H^-$  production coefficient  $K^- = I_{H^--cnv}/I^+$  may vary from .1 to .7 in cesiated SPS[6].  $I_{H^--cnv}$  is the  $H^-$  current produced at the converter. Since  $I_{cnv} = I^+ + I^- = 4A$ , a prediction for possible  $I_{H^--cnv}$  may be made over the limits of the  $\gamma$  and  $K^-$

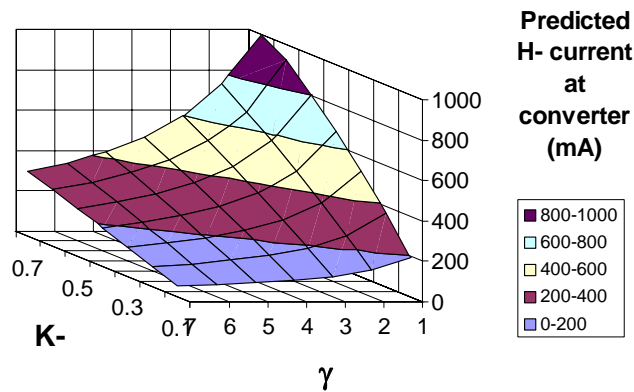


Fig. 11. Prediction for  $H^-$  converter current,  $I_{H^--cnv}$ , using the measured converter current,  $I_{cnv}$  of 4A, and published  $\gamma$  and  $K^-$  factors for SPS.

parameters. Here  $I^- = (\gamma + K^-)I^+$ . The prediction is shown in Fig. 11, and  $(I_{H^--cnv})_{min} = 40mA$  is found at  $\gamma = 7$ ,  $K^- = 0.1$  while  $(I_{H^--cnv})_{max} = 1000mA$  is found for  $\gamma = 1$ ,  $K^- = 0.7$ . For a well-cesiated molybdenum surface the parameters  $\gamma$  and  $K^-$  may be 7 and 0.7[6] which yields  $I_{H^--cnv} = 300mA$ . This  $H^-$  converter current is order factor ten greater than the PBGUNS sputter model currents used in Fig 8(A).

In addition to  $H^-$  sputter energy at the converter, another cause of converter efficiency reduction is  $H^-$  converter beam expansion by incomplete neutralization of the  $H^-$  beam space charge. Such expansion may occur in a localized area around the converter sheath, and/or in beam transport from the converter to the emission aperture. An approximate plasma density of  $10^{11} (cm)^{-3}$  has been derived in the six-filament source by using the converter as a floating probe. Using this plasma density and an assumed electron temperature of 1eV, a converter plasma sheath thickness of 1.7 mm is derived[19]. A 2-D particle in cell (PIC) code is being developed at Los Alamos for application to ion source plasma problems[20]. A preliminary result from the PIC code simulation as applied to this  $H^-$  surface conversion source is shown in Fig. 12.

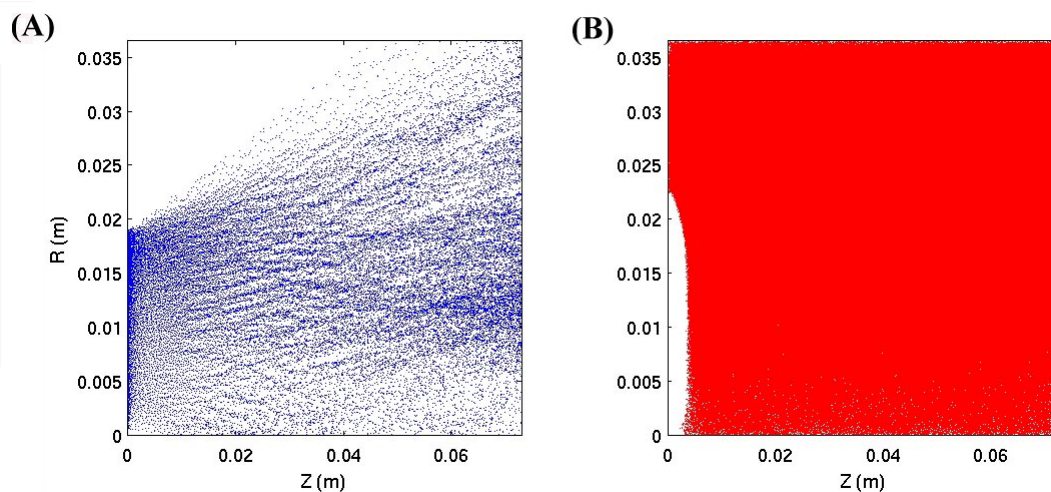


Fig. 12. Preliminary 2-D PIC code simulation for  $H^-$  beam being accelerated off the surface converter located on the left in Figs. 12(A). Fig. 12(B) shows the plasma electrons, and formation of the sheath at about 3 mm from the converter.

The plasma density in this simulation is  $3 \times 10^{10} \text{ (cm)}^{-3}$ . The  $H^-$  beam is born on the plasma converter on the left of Fig. 12(A). The sheath region shown in Fig. 12(B) has formed approximately 3mm downstream from the converter. The 300eV  $H^-$  beam is indeed predicted to have a strong divergence at the converter from residual negative space-charge, and from a defocusing electric field at the converter edge. These sheath predictions are suggestive of further experimental work with shaped converters. Not until experiments on electron repeller options and increased  $H^-$  production efficiency are completed, will the parameters labeled TBD in Table 1 be established.

## ACKNOWLEDGEMENTS

We acknowledge the U.S. National Nuclear Security Administration (NNSA) and LANSCE Division operations for continued support in the field of  $H^-$  source development.

## REFERENCES

1. Benjamin A. Prichard, Jr., and Ralph R. Stevens, Jr., "Status of the SPSS  $H^-$  Ion Source Development Program", Los Alamos National Lab Report LA-UR-02-547 (2002).
2. G. Rouleau, E. Chacon-Golcher, E. G. Jacobson, B. J. Meyer, and E. G. Geros, B. A. Prichard, Jr., J. D. Sherman, J. E. Stelzer, R. R. Stevens, Jr., " $H^-$  Surface Converter Source Development at Los Alamos", Proceedings of the 2003 Particle Accelerator Conference (Portland, Oregon), IEEE Catalog Number 03CH37423C, 73 (2003).
3. J. Sherman, A. Arvin, E. Chacon-Golcher, E. Geros, E. Jacobson, B. Meyer, P. Naffziger, G. Rouleau, S. Schaller, J. Stelzer, and T. Zaugg, "Development of a 25-mA, 12% Duty Factor  $H^-$  Source for LANSCE", to be published in Proc. of the 2004 European Particle Accelerator Conference (Lucerne, Switzerland).
4. R. Keller, J. M. Verbeke, P. Scott, M. Wilcox, L. Wu, and N. Zahir, "A Versatile Column Layout for the LANSCE Upgrade", Proceedings of the 1999 Particle Accelerator Conference (New York), IEEE Catalog Number 99CH36366, 1926 (1999).

5. R. R. Stevens, Jr., W. Ingalls, O. Sander, B. Prichard, and J. Sherman, "Beam Simulations for the H<sup>-</sup> Injector Upgrade at LANSCE", Proc. of the XIX International Linac Conference (Chicago, IL), Argonne National Lab Report ANL-98/28, 514 (1998).
6. Yu. I. Belchenko, G. I. Dimov, and V. G. Dudnikov, "Physical Principles of the Surface Plasma Method for Producing Beams of Negative Ions", Proc. of the Symposium on the Production and Neutralization of Negative Hydrogen Ions and Beams (Brookhaven, New York), Brookhaven National Lab Report BNL 50727, 79(1977).
7. W. B. Ingalls, M. W. Hardy, B. A. Prichard, O. R. Sander, J. E. Stelzer, R. R. Stevens, K. N. Leung, and M. D. Williams, "Enhanced H<sup>-</sup> Ion Source Testing Capabilities at LANSCE", Proc. of the XIX International Linac Conference (Chicago, IL), Argonne National Lab Report ANL-98/28, 887 (1998).
8. R. C. McCrady, M. S. Gulley, and A. A. Browman, "Evaluation of the LANSCE H<sup>-</sup> Low-Energy Beam Transport System for High Emittance Beams", LANSCE Activity Report LA-13943-PR, 58(2001).
9. Jack E. Boers, "PBGUNS: An Interactive IBM PC Computer Program for the Simulation of Electron and Ion Beams and Guns", Thunderbird Simulations, (August, 2001).
10. R. F. Welton, M. P. Stockli, J. E. Boers, R. Rauniyar, R. Keller, J. W. Staples, and R. W. Thomae, "Simulation of the Ion Source Extraction and Low Energy Beam Transport Systems for the Spallation Neutron Source", Review of Sci. Instrum. 73 (2), 1013(2002).
11. J. Guyard and M. Weiss, Proc. of the 1976 Linear Accelerator Conf., (Chalk River, Ontario, Canada), AECL-5677, 254(1976).
12. Ralph R. Stevens, Jr., Rob L. York, John R. McConnell, and Robert Kandarian, "Status of the High-Intensity H<sup>-</sup> Injector at LAMPF", Proc of the 1984 Linear Accelerator Conf., (Seeheim, Germany), GSI-84-11, 226(1984).
13. R. L. York, Ralph R. Stevens, Jr., R. A. Dehaven, J. R. McConnell, E. P. Chamberlain, and R. Kandarian, Nucl. Instrum. And Methods in Phys. Res. B10/11, 891(1985).
14. J. W. Kwan, G. D. Ackerman, O. A. Anderson, C. F. Chan, W. S. Cooper, G. J. DeVries, A. F. Lietzke, L. Soroka, and W. F. Steele, Rev. Sci. Instrum 57(5), 831(1986).
15. K. W. Ehlers and K. N. Leung, "Electron Suppression in a Multicusp Negative Ion Source", Appl. Phys. Lett.38 (4), 287(1981).
16. Dan M. Goebel, "Ion Source Discharge Performance and Stability", Phys. Fluids 25(6), 1093(1982).
17. A. P. H. Goede and T. S. Green, "Operation Limits of Multipole Ion Sources", Phys. Fluids 25(10), 1797(1982).
18. Vadim Dudnikov, Rev. Sci. Instrum. 73(2) (Feb. 2002), 992.
19. Claude LeJeune, Advances in Electronics and Electron Physics, Academic Press, Part C, Very High Density Beams (1983), 207.
20. Edwin Chacon-Golcher, K. J. Bowers, and J. D. Sherman, "Progress in the Computer Simulation of LANSCE's Production H<sup>-</sup> Source", to be published in the Proc. of the 31<sup>st</sup> European Plasma Physics Physical Society (London, England), (June, 2004)